Table 2. Rate constants for the quenching of **1** by pyridinium ion acceptors Q^+ in degassed acetone (0.1 M NBu_4PF_6) at 25 °C.

Quencher [a]	$E(Q^+/Q^0)$/V [b]	k_q'/L mol^{-1} s^{-1} [c]
3,4-dicyano-*N*-methylpyridinium	−0.11	4.05×10^9
2-chloro-*N*-methyl-3-nitropyridinium	−0.37	7.78×10^9
4-cyano-*N*-methylpyridinium	−0.67	5.23×10^9
4-methoxycarbonyl-*N*-methylpyridinium	−0.78	2.59×10^9
4-aminoformyl-*N*-ethylpyridinium	−0.93	9.17×10^8
3-aminoformyl-*N*-methylpyridinium	−1.14	9.56×10^7
N-ethylpyridinium	−1.36	1.13×10^7
4-methyl-*N*-methylpyridinium	−1.49	1.47×10^6

[a] All the cations have hexafluorophosphate counterions except for 3,4-dicyano-*N*-methylpyridinium and 2-chloro-*N*-methyl-3-nitropyridinium which have tetrafluoroborate counterions. [b] Measured against the saturated sodium chloride calomel electrode. [c] k_q' is the rate constant corrected for diffusional effects.

Experimental Procedure

1: To a solution of trimethylsilylacetylene (0.04 mL, 0.30 mmol) in pre-dried, degassed THF (40 mL) under an inert atmosphere of nitrogen, *n*-butyllithium (1.6 M, 0.18 mL, 0.30 mmol) was added at room temperature. A solid sample of $[Cu_2(\mu\text{-dppm})_2(MeCN)_2](BF_4)_2$ (500 mg, 0.43 mmol) was added and stirred at room temperature for 24 h. After evaporation to dryness, the resulting solid was extracted with acetone (3 × 8mL), and the solution was filtered and reduced in volume. Subsequent layering of *n*-hexane into the concentrated solution gave **1** as air-stable pale yellow crystals (yield 200 mg, 46%). ^{1}H NMR (270 MHz, [D$_6$]acetone, 25 °C, relative to TMS): δ = 3.74 (m, 8H; CH_2), 7.00–7.43 (m, 80H; Ph); IR (nujol/KBr): ν[cm^{-1}]: 1057 s, (ν (B–F)); UV/Vis (acetone): λ[nm] (ε_{max}/L mol^{-1}cm^{-1}) = 374 (7420); positive ion FAB-MS: ion cluster at *m/z* 1901 [M^+]. Anal. calcd for $C_{102}H_{88}P_8B_2F_8Cu_4 \cdot H_2O$: C 61.03, H 4.42; found: C 61.13, H 4.45.

Received: December 22, 1995 [Z8678IE]
German version: *Angew. Chem.* **1996**, *108*, 1213–1215

Keywords: bridging ligands · complexes with carbon ligands · coordination · copper compounds · luminescence

[1] T. B. Marder, G. Lesley, Z. Yuan, H. B. Fyfe, P. Chow, G. Stringer, I. R. Jobe, N. J. Taylor, I. D. Williams, S. K. Kurtz, *ACS Symp. Ser.* **1991**, *455*, 605; see also N. J. Long, *Angew. Chem.* **1995**, *107*, 37–56; *Angew. Chem. Int. Ed. Engl.* **1995**, *34*, 21–38.

[2] E. Sappa, A. Tiripicchio, P. Braunstein, *Coord. Chem. Rev.* **1985**, *65*, 219.

[3] R. Nast, *Coord. Chem. Rev.* **1982**, *47*, 89.

[4] V. W. W. Yam, W. K. Lee, T. F. Lai, *Organometallics* **1993**, *12*, 2383; V. W. W. Yam, W. K. Lee, P. K. Y. Yeung, *J. Phys. Chem.* **1994**, *98*, 7545; V. W. W. Yam, W. K. Lee, *J. Chem. Soc. Dalton Trans.* **1993**, 2097; V. W. W. Yam, S. W. K. Choi, *ibid.* **1994**, 2057.

[5] V. W. W. Yam, W. K. Lee, T. F. Lai, *J. Chem. Soc. Chem. Commun.* **1993**, 1571.

[6] a) Crystal Data of **1**: $[(Cu_4P_8C_{102}H_{88})^{2+} \cdot 2BF_4^- \cdot 4(CH_3)_2CO]$, formula weight = 2221.72, orthorhombic, space group *Pccn* (no. 56), a = 21.290(1), b = 23.019(1), c = 22.882(2) Å, V = 11213.7(10) Å^3, Z = 4, ρ_{calcd} = 1.316 g cm^{-3}, $\mu(Mo_{K\alpha})$ = 9.25 cm^{-1}, $F(000)$ = 4576, T = 298 K. A pale yellow crystal of dimensions 0.20 × 0.15 × 0.30 mm mounted inside a capillary glass tube in the presence of some solvent was used for data collection at 25 °C on a Rigaku AFC7R diffractometer with graphite monochromatized $Mo_{K\alpha}$ radiation (λ = 0.71073 Å). ω-2θ scans were used with ω scan angle (0.63 + 0.35 tanθ) at a scan speed of 16.0° min^{-1} (up to four scans for reflections with $I < 15\sigma(I)$). Intensity data (in the range of $2\theta_{max}$ = 45°; h: 0 to 24; k: 0 to 25; l: 0 to 23 and three standard reflections measured after every 300 reflections showed no decay) were corrected for Lorentz and polarization effects, and empirical absorption corrections based on the ψ scan of four strong reflections (minimum and maximum transmission factors 0.925 and 1.000). 8022 reflections were measured, 3357 reflections with $I > 3\sigma(I)$ were considered observed and used in the structural analysis. The space group was determined from systematic absences and the structure was solved by Patterson methods and expanded by Fourier methods (PATTY [6b]) and refinement by full-matrix least squares by using the software package TeXsan [6c] on a Silicon Graphics Indy computer. Only the six heavy atoms (copper and phosphorus) were refined anisotropically. The other 65 non-hydrogen atoms were refined isotropically. 56 hydrogen atoms at calculated positions with thermal parameters equal to 1.3 times that of the attached C atoms were not refined. Convergence for 311 variable parameters by least squares refinement on F with $w = 4F_o^2/\sigma^2(F_o^2)$, where $\sigma^2(F_o^2) = [\sigma^2(I) + (0.012F_o^2)^2]$ for 3357 reflections with $I > 3\sigma(I)$ was reached at R = 0.074 and wR = 0.085 with a goodness-of-fit of 3.00. $(\Delta/\sigma)_{max}$ = 0.04 for the complex cation. Crystallographic data (excluding structure factors) for the structure(s) reported in this paper have been deposited with the Cambridge Crystallographic Data Centre as supplementary publication no. CCDC-179-23. Copies of the data can be obtained free of charge on application to The Director, CCDC, 12 Union Road, Cambridge CB2 1EZ, UK (fax: Int. code + (1223) 336-033; e-mail teched@chemcrys.cam.ac.uk). b) PATTY: P. T. Beurskens, G. Admiraal, G. Beurskens, W. P. Bosman, S. Garcia-Granda, R. O. Gould, J. M. M. Smits, C. Smykalla, **1992**. The DIRDIF program system, Technical Report of the Crystallography Laboratory, University of Nijmegen, The Netherlands; c) TeXsan: Crystal Structure Analysis Package, Molecular Structure Corporation, **1985** and **1992**.

[7] a) M. I. Bruce, M. R. Snow, E. R. T. Tiekink, M. L. Williams, *J. Chem. Soc. Chem. Commun.* **1986**, 701; b) M. G. B. Drew, F. S. Esho, S. M. Nelson, *J. Chem. Soc. Chem. Commun.* **1982**, 1347.

[8] J. C. Slater, *J. Chem. Phys.* **1964**, *41*, 3199.

[9] P. Braunstein, M. A. Luke, A. Tiripicchio, M. T. Camellini, *Angew. Chem.* **1987**, *99*, 802–803; *Angew. Chem. Int. Ed. Engl.* **1987**, *26*, 768–770.

Mesoporous Alumina Molecular Sieves**

Stephen A. Bagshaw and Thomas J. Pinnavaia*

The original synthesis of Mobil M41S mesoporous molecular sieves[1, 2] utilized electrostatic interactions between a positively charged surfactant (S^+) and a negatively charged inorganic precursor (I^-) to assemble the mesostructure. The electrostatic assembly process has been verified[3, 4] and extended to include charge-reversed (S^-I^+) and counterion-mediated ($S^-M^+I^-$ and $S^+X^-I^+$; M^+ = metal cation, X^-) pathways.[5–7] We recently demonstrated that mesostructure assembly, at least in the case of silica, can also be achieved through hydrogen bonding interactions between neutral inorganic precursors (I^0) and neutral alkylamine (S^0) or nonionic polyethylene oxide (N^0) surfactants.[8, 9] More recently, Attard et al.[10] have shown that N^0 surfactants in liquid crystalline form function as authentic templates for the synthesis of M41S silicas with hexagonal, cubic, and lamellar structure. Neutral S^0I^0 and N^0I^0 pathways have important advantages over the electrostatic pathways, in part, because most metals form alkoxides or other neutral complexes suitable for hydrolysis and assembly as I^0 precursors. The diversity of compositions of I^0 precursors allows for the synthesis of mesostructured oxides that are difficult or impossible to achieve by electrostatic assembly mechanisms. We describe here the application of the concept of neutral surfactant templating to the synthesis of the first examples of alumina molecular sieves.

High surface area aluminas are especially important industrial catalysts and catalyst supports.[11, 12] Yet, the performance properties of these widely used phases undoubtedly is limited, because they possess only textural porosity and lack the selective framework/confined pore structure characteristic of a molecular sieve. There have been previous attempts to prepare mesostructured forms of alumina by electrostatic assembly pathways,[5–7] but all afforded products that collapsed upon surfactant removal. However, as shown by the present work, N^0I^0 assembly processes provide highly effective pathways to mesoporous alumina molecular sieves.

[*] Prof. T. J. Pinnavaia, Dr. S. A. Bagshaw
Department of Chemistry and Center for Fundamental Materials Research
Michigan State University
East Lansing, MI 48824 (USA)
Fax: Int. code + (517)432-1225
e-mail: Pinnavaia@cemvax.cem.msu.edu

[**] The support of this research by the National Science Foundation through Chemistry Group Grant CHE-9224102 is gratefully acknowledged.

Table 1. Properties of MSU-X mesoporous alumina molecular sieves calcined at 773 K.

Material designation	Template	Surfactant formulae	Amount of template [a] [mmol]	Surface area [$m^2 g^{-1}$]	d_{100} [nm]	HK pore size [nm]	BJH pore size [nm]	Mesopore volume [b] [mL g^{-1}]
MSU-1	Tergitol 15-S-9 [c]	$C_{11-15}[EO]_9$	10.7	490	8.0	5.5	3.3	0.40
	Tergitol 15-S-12	$C_{11-15}[EO]_{12}$	8.5	425	8.5	6.5	3.5	0.44
	Tergitol 15-S-20	$C_{11-15}[EO]_{20}$	5.8	535	9.0	7.0	4.6	0.68
MSU-2	Igepal RC-760 [d]	$C_{12}Ph[EO]_{18}$	5.9	420	9.6	8.0	4.7	0.64
	Triton X-114 [e]	$C_8Ph[EO]_8$	9.0	460	>9.0	8.0	3.3	0.35
	Triton X-100	$C_8Ph[EO]_{10}$	11.2	445	>9.0	8.0	3.6	0.37
MSU-3	Pluronic 64 L [f]	$[PEO]_{13}[PPO]_{30}[PEO]_{13}$	2.1	430	6.8	4.0	2.4	0.21

[a] All syntheses were performed at a surfactant concentration of 25 wt%. [b] Mesopore volume for pores between 2.0 and 8.0 nm diameter according to the BJH analyses. [c] Tergitol 15-S-x surfactants kindly supplied by Union Carbide. [d] Igepal RC-760 kindly supplied by Rhone-Poulenc. [e] Triton-X surfactants supplied by Aldrich. [f] Pluronic 64 L kindly supplied by BASF.

Three forms of mesoporous aluminas, denoted MSU-1, MSU-2, and MSU-3, were prepared by the hydrolysis of tri-*sec*-butoxyaluminum at ambient temperature in the presence of the nonionic polyethylene oxide surfactants given in Table 1. Typical powder X-ray diffraction (XRD) patterns are shown in Figure 1 for the as-synthesized and calcined forms of MSU-3 alumina prepared from a copolymer surfactant of the type $(PEO)_{13}(PPO)_{30}(PEO)_{13}$ based on polyethylene oxide (PEO) and polypropylene oxide (PPO). Analogous single peak patterns corresponding to large d spacings have been observed for disordered MCM-41,[3, 5] HMS,[8] and MSU-X[9] silicas. However, the reflections for MSU-X aluminas are broader, signifying an even greater degree of structural disorder. Also, the intensities of the XRD lines are substantially larger for the calcined forms of MSU aluminas than for the as-synthesized materials. Analogous changes in XRD intensities have been observed for MCM-41 and HMS silicas.[9] Recent modeling studies by S. D. Mahanti[13] have shown that the removal of the occluded organic template from hexagonal mesostructures enhances the Bragg scattering cross-section. Similar differences in scattering intensities are anticipated for as-synthesized and calcined forms of disordered mesostructures.

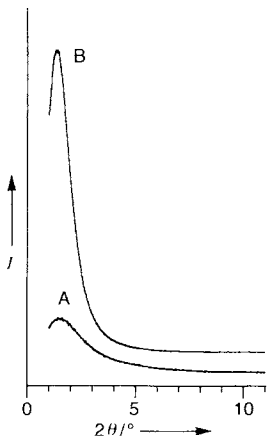

Fig. 1. Powder X-ray diffraction patterns of MSU-3 alumina prepared with Pluronic 64L surfactant: A) As-synthesized sample after air drying at room temperature for 16 h; B) after calcination at 773 K in air for 6 h. The intensity I is in arbitrary units.

PEO-based surfactants are known to adopt spherical to long "wormlike" micellar structures in aqueous solution.[14–16] The pore structures of MSU-X aluminas prepared with these N^0 surfactants reflect the wormlike motif of the micellar structure, as evidenced by the representative transmission electron microscopic (TEM) image (Fig. 2) for a MSU-1 alumina prepared from Tergitol 15-S-9. However, the wormlike channels, though more or less regular in diameter, have no discernible long-range order. That is, the packing of channel system appears to be random, despite the presence of an XRD reflection. In this latter case the regular separation between single channel walls may be giving rise to the XRD reflection. Clearly, the disordered channel system of MSU-X aluminas is in marked contrast to the long-range hexagonal arrangement of channels found for MCM-41[2] and HMS mesostructures.[8]

Fig. 2. TEM image of a calcined (773 K) MSU-1 alumina molecular sieve showing the regular wormlike channel motif, but no discernable long-range channel packing order. The material was prepared by using Tergitol 15-S-9 as the surfactant. The length of the bar corresponds to 60 nm.

Figure 3 provides representative N_2 adsorption/desorption isotherms for a MSU-3 alumina calcined at 773 K. All MSU-X aluminas prepared by using PEO surfactants as templates display a similar broad but well-defined step in the adsorption isotherm at $p/p_0 \approx 0.45-0.8$ and a hysteresis in the desorption isotherm over the same relative pressure range. These features result from the condensation of the adsorbate within the framework-confined mesopores,[17] not from interparticle pores.[18] The lack of textural mesoporosity is indicated further by the absence of a hysteresis loop above $p/p_0 = 0.8$.[8] Some necking of the pore structure is suggested by the sharp curvature in the desorption leg of the hysteresis loop.

Most previously reported studies of mesoporous molecular sieves[1–9] have made use of the Horvath–Kawazoe (HK) model[19] for the determination of pore size distributions from N_2 adsorption isotherms. This model, developed for microporous lamellar carbon materials, assumes the presence of slitlike micropores. Therefore, its applicability to materials with larger,

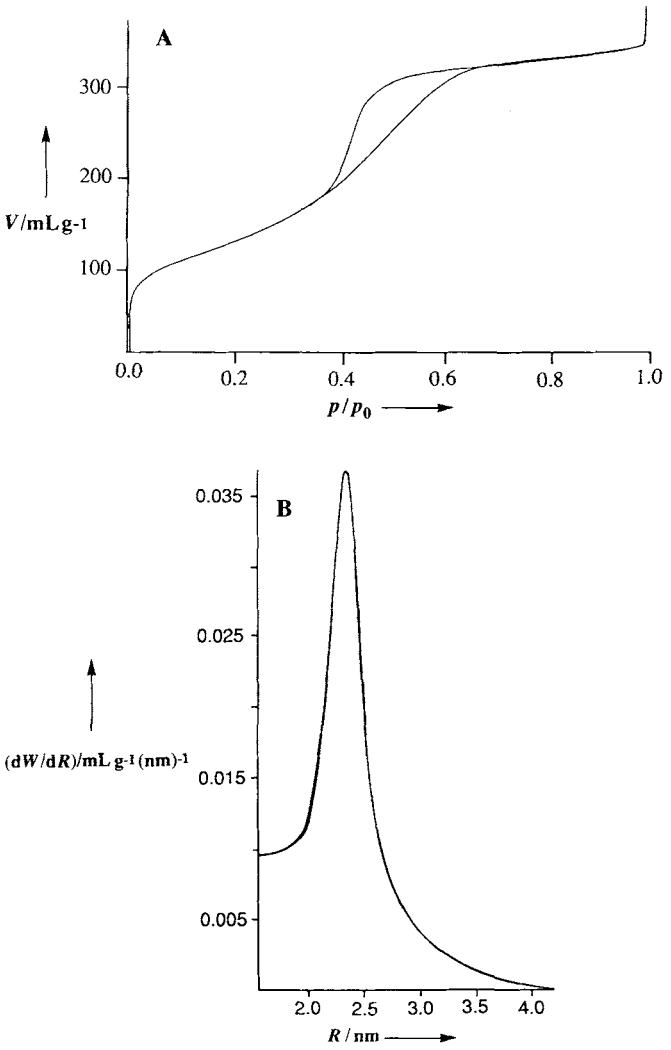

Fig. 3. A) Nitrogen adsorption and desorption isotherms for MSU-3 alumina prepared with the Pluronic 64L surfactant and calcined at 773 K in air for 4 h. The volume of N_2 sorbed is expressed at standard temperature and pressure; p/p_o is the partial pressure of nitrogen in equilibrium with the sample at 77 K. B) Corresponding Barrett–Joiner–Halender pore size distribution determined from the N_2 adsorption isotherm. dW/dR is the derivative of the normalized N_2 volume adsorbed with respect to the diameter of the pores of the adsorbent. Prior to measurement the sample was evacuated at 423 K and 10^{-6} Torr for 16 h.

cylindrical mesopores is likely to be limited. In this report, we have applied in addition to the HK model both the Cranston–Inkley (CI)[20] and the Barrett–Joyner–Halender (BJH)[21] models to the determination of framework pore size. Comparable pore size values were obtained when the CI and BJH models were applied to the N_2 adsorption and desorption branches, respectively. However, HK gave significantly larger pore diameters. For instance, as shown in Figure 3B, the pore distribution determined by the BJH method for MSU-3 alumina is centered at 2.4 nm, whereas the HK model affords a value of 4.8 nm. Measurement of the pores in the TEM image in Figure 2 gave diameters of about 2.6 nm, a value in favorable agreement with the BJH value of 3.3 nm.

Table 1 gives the basal spacings d_{100}, surface areas, pore volumes, and the HK and BJH pore sizes for MSU-X aluminas prepared from different families of PEO-based surfactants. A mesostructure assembly effect is indicated by an increase in both the d spacing and the pore diameters with increasing surfactant size. Since the MSU-X aluminas exhibit similar pore sizes but larger d spacings than MSU-X silicas,[9] we conclude that the channel wall thicknesses is larger for the aluminas than the silicas. This is consistent with the observation that the Brunauer–Emmett–Teller (BET)[18] surface areas of the aluminas calcined in air at 773 K range from 420 to 535 $m^2 g^{-1}$, whereas MSU-X silicas give values twice as large. Nevertheless, the surface areas and pore volumes are substantially larger than those of amorphous and crystalline aluminas[22] prepared by traditional sol–gel or flash-calcination techniques.[23]

The coordination environment of aluminum in MSU-X aluminas was examined by ^{27}Al MAS NMR spectroscopy (MAS = magic angle spinning). Spectra of as-synthesized and calcined MSU-3 alumina (Fig. 4) display three resonance signals, uncorrected for quadrupolar shift, at $\delta = 0$, 35, and 75. These lines are indicative of six-, five-, and four-coordinate metal centers, respectively.[24, 25] In the as-synthesized material the six-coordinate species is dominant, but after dehydration and dehydroxylation at 773 K the four- and five-coordinate centers both increase at the expense of the six-coordinate centers. The presence of five-coordinate aluminum centers is especially noteworthy as they may prove to be of catalytic significance as Lewis acid centers.

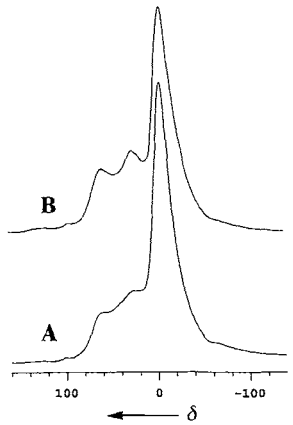

Fig. 4. ^{27}Al MAS NMR spectra of MSU-3 alumina prepared with the Pluronic 64L surfactant: A) As-synthesized sample after air drying at room temperature for 16 h; B) after calcination at 773 K in air for 4 h. The chemical shifts are referenced to external $[Al(H_2O)_6]^{3+}$.

Finally, we note that porous aluminas[26, 27] and aluminates[28] have been prepared previously from alkoxide precursors in the presence of organic pore regulating agents such as methyl cellulose or short-chain quaternary ammonium cations. Although these organic modifiers exhibited structure-directing properties for zeolite syntheses,[29] they afforded aluminas that were X-ray amorphous. Consequently, these earlier alumina synthesis reactions involved modifier encapsulation, but not assembly processes. Alumina aerogels with surface areas near 500 $m^2 g^{-1}$ also have been reported,[30] but the pore structures of these low bulk density materials were purely textural. Because of their thermal stability, high surface area, and multiple aluminum coordination environments, MSU-X alumina molecular sieves offer promising opportunities for new materials applications, particularly as catalysts and catalyst supports.

Experimental Procedure

The synthesis of a representative product, MSU-3 alumina, prepared by using a polyethylene oxide/polypropylene oxide copolymer surfactant illustrates the general procedure for the preparation of a mesoporous alumina molecular sieve. The specific template employed was Pluronic 64L (BASF), a tri-block copolymer with specific stoichiometry $(PEO)_{13}(PPO)_{30}(PEO)_{13}$. A solution containing deionized water (42 mmol) in anhydrous *sec*-butyl alcohol (10 mL) was added very slowly ($\approx$1 mL min^{-1}) to a stirred homogeneous solution containing surfactant (2.1 mmol) and tri-*sec*-butoxyaluminum (21 mmol) in anhydrous *sec*-butyl alcohol (25 mL). The overall reaction stoichiometry, therefore, was 0.1:1.0:2.0 surfactant:Al:water. The resulting gel that formed after stirring for 3 h was diluted with *sec*-butyl alcohol and allowed to react for an additional 16 h. The product was washed with absolute ethanol and dried sequentially at room temperature for 16 h and at 373 K for 6 h. The calcination was carried out by heating to 773 K for 4 h.

XRD patterns were obtained with a Rigaku Rotaflex diffractometer equipped with a rotating anode and $Cu_{K\alpha}$ radiation ($\lambda = 0.15418$ nm). The TEM image was obtained with a JEOL 100CX microscope using an accelerating voltage of 120 kV and a 20 mm objective lens aperture. N_2 isotherms were obtained on a Coulter Om-

  0570-0833/96/3510-1104 $ 15.00+.25/0

nisorp 360CX Sorptometer operated under continuous adsorption conditions. ^{27}Al MAS NMR spectra were obtained with a Varian VXR-400 NMR spectrometer equipped with a Varian MAS probe and SiN rotor. The spectrometer frequency was 104.22 MHz, pulse width 2 ms, and sample spinning rate 6550 Hz.

Received: November 17, 1995
Revised version: February 14, 1996 [Z8563IE]
German version: *Angew. Chem.* **1996**, *108*, 1180–1183

Keywords: aluminum compounds · mesoporous materials · molecular sieves · surfactants

[1] J. S. Beck, *US-A* 5057296, **1991**.
[2] C. T. Kresge, M. E. Leonowicz, W. J. Roth, J. C. Vartuli, J. S. Beck, *Nature* **1992**, *359*, 710.
[3] C.-Y. Chen, H.-Y. Li, M. E. Davis, *Microporous Mater.* **1993**, *2*, 17.
[4] C.-Y. Chen, H.-Y. Li, S. L. Burkett, M. E. Davis, *Microporous Mater.* **1993**, *2*, 27.
[5] Q. Huo, D. I. Margolese, U. Ciesla, D. G. Demuth, P. Feng, T. E. Gier, P. Sieger, A. Firouzi, B. F. Chmelka, F. Schüth, G. Stucky, *Chem. Mater.* **1994**, *6*, 1176.
[6] Q. Huo, D. I. Margolese, U. Ciesla, P. Feng, T. E. Gier, P. Sieger, R. Leon, P. M. Petroff, F. Schüth, G. Stucky, *Nature* **1994**, *368*, 317.
[7] U. Ciesla, D. Demuth, R. Leon, P. Petroff, G. Stucky, K. Unger, F. Schüth, *J. Chem. Soc. Chem. Commun.* **1994**, 1387.
[8] P. T. Tanev, T. J. Pinnavaia, *Science* **1995**, *267*, 865.
[9] S. A. Bagshaw, E. Prouzet, T. J. Pinnavaia, *Science* **1995**, *269*, 1242.
[10] G. S. Attard, J. C. Glyde, C. G. Göltner, *Nature* **1995**, *378*, 366.
[11] C. Misra, *Industrial Alumina Catalysts*, ACS Monograph Series **1986**, *184*, 133.
[12] G. Tournier, M. Lecroix-Repellin, G. M. Pajonk, *Stud. Surf. Sci. Catal.* **1987**, *31*, 333.
[13] S. D. Mahanti, personal communication.
[14] M. R. Porter, *Handbook of Surfactants*, 2nd ed., Blackie, London, **1994**.
[15] B. Chu, *Langmuir* **1995**, *11*, 414.
[16] Z. Lin, L. E. Scriven, H. T. Davis, *Langmuir* **1992**, *8*, 2200.
[17] P. J. Branton, P. G. Hall, K. S. W. Sing, H. Reichert, F. Schüth, K. K. Unger, *J. Chem. Soc. Faraday Trans.* **1994**, *90*, 2965.
[18] S. J. Gregg, K. S. W. Sing, *Adsorption, Surface Area and Porosity*, 2nd ed., Academic Press, London, **1982**.
[19] G. Horvath, J. Kawazoe, *J. Chem. Eng. Jpn.* **1983**, *16*, 470.
[20] R. W. Cranston, F. A. Inkley, *Adv. Catal.* **1970**, *9*, 143.
[21] E. P. Barrett, L. G. Joyner, P. P. Halender, *J. Am. Chem. Soc.* **1951**, *73*, 373.
[22] R. Poisson, J.-P. Brunelle, P. Nortier in *Catalyst Supports and Supported Catalysts*, (Ed.: A. B. Stiles), Butterworths, Boston, **1987**, p. 11.
[23] B. C. Gates in *Materials Chemistry: An Emerging Discipline*, American Chemical Society, Washington, D. C., **1995**, p. 301.
[24] J. W. Akitt, *Prog. Nucl. Magn. Reson. Spectrosc.* **1989**, *21*, 127.
[25] M. C. Cruickshank, L. S. Dent Glasser, S. A. I. Barri, I. J. Proplett, *J. Chem. Soc. Chem. Commun.* **1986**, 23.
[26] H. Adkins, S. H. Watkins, *J. Am. Chem. Soc.* **1951**, *73*, 2184.
[27] D. Basmadjian, G. Fulford, B. I. Parsons, D. S. Montgomery, *J. Catal.* **1962**, *1*, 547.
[28] R. Sned, *Appl. Catal.* **1984**, *12*, 347.
[29] *Introduction to Zeolite Science and Practice*, (Eds.: H. van Bekkum, E. M. Flanigen, J. C. Jansen) Elsevier, Amsterdam, **1991**.
[30] C.-M. Chen, S.-Y. Chen, S.-Y. Peng, *Studi. Surf. Sci. Catal.* **1995**, *91*, 427.

Design, Synthesis, and Ion-Transport Properties of a Novel Family of Cyclic, Adamantane-Containing Cystine Peptides**

Darshan Ranganathan,* V. Haridas, K. P. Madhusudanan, Raja Roy, R. Nagaraj, G. B. John, and M. B. Sukhaswami

Cyclic peptides have attracted considerable attention in recent years. Apart from acting as templates in the de novo design[1] of artificial proteins, they serve as useful models[2] for the study of preferences in protein secondary structure and also play a pivotal role in ion transport across biological membranes.[3] Recently, a new aspect has developed: the formation of nanotubes from cyclic peptides.[4]

The problem of delineating conformation in cyclic peptides can be overcome by incorporating rigid units in their framework. The potential of this strategy has recently been shown in the design of conformationally constrained, high-affinity ligands for GPIIb/IIIb receptor proteins[5] and in the development of minimal glucocorticoid receptors models.[6] Thus, it was envisaged that when rigid and simultaneously lipophilic units are incorporated into the cyclic peptide framework, not only would the peptide have the desired conformational constraint but it would also interact with lipid bilayers. These cyclic peptides would thereby effectively and preferentially transport ions across biological membranes.

In this communication we provide the first illustration of this strategy and report on the design and synthesis of a unique family of adamantane-containing[7] cystine cyclic peptides with the general structure cyclo(Adm-Cyst)$_n$ (Adm = 1,3-adamantanedicarbonyl; Cyst = L-cystine dimethyl ester; $n = 2-5$), which were constructed in a single step by the reaction of L-cystine dimethyl ester with 1,3-adamantanedicarbonyl dichloride. Further, members of this class of cyclic peptides have been demonstrated to selectively transport sodium and potassium ions in model membranes.

Treatment of 1,3-adamantane dicarbonyl dichloride with L-cystine dimethyl ester in the presence of triethylamine under high-dilution conditions afforded a mixture of four products with similar TLC behavior, which were separated by chromatography on silica gel with ethyl acetate/benzene (80/20) as eluent. The products were isolated in yields of 55 (**1**), 15 (**2**), 12 (**3**), and 2% (**4**), and were fully characterized by spectroscopic and analytical data (Scheme 1, Table 1)).

The highly symmetrical nature of **1**–**4** was evident from the appearance of only single set of resonances for the cystine and adamantane units in their ^{1}H and ^{13}C NMR spectra.[15] The chemical shifts of the adamantane and cystine protons in **2**–**4** were essentially identical to those of **1**, suggesting that these units adopt similar conformations. The ROESY NMR spectra of **1**–**3** and the very enhanced ROE effect[15] between the NH and the adamantane methylene protons suggests that

[*] Dr. D. Ranganathan, V. Haridas
Biomolecular Research Unit, Regional Research Laboratory (CSIR)
Trivandrum, 695019 (India)
Fax: Int. code +(471)490186
Dr. K. P. Madhusudanan, Dr. R. Roy
Medicinal Chemistry Division, Central Drug Research Institute
Lucknow, 226001 (India)
Dr. R. Nagaraj, G. B. John, Dr. M. B. Sukhaswami
Centre for Cellular and Molecular Biology, Hyderabad (India)

[**] This work was supported financially by the Department of Science and Technology, New Delhi (India). We are most grateful to Prof. S. Ranganathan (RRL, Trivandrum) and Prof. D. Balasubramanian (CCMB, Hyderabad) for helpful advice and comments.

  0570-0833/96/3510-1105 $ 15.00+.25/0